Inorganic Chemistry

Article

pubs.acs.org/IC

Enhancing Photoluminescence Performance of $SrSi_2O_2N_2:Eu^{2+}$ Phosphors by Re (Re = La, Gd, Y, Dy, Lu, Sc) Substitution and Its Thermal Quenching Behavior Investigation

Wei Lü,*[,†] Mengmeng Jiao,[†,‡] Baiqi Shao,[†,‡] Lingfei Zhao,[†,‡] and Hongpeng You*[,†]

[†]State Key Laboratory of Rare Earth Resource Utilization, Changchun Institute of Applied Chemistry, Chinese Academy of Sciences, Changchun 130022, P. R. China

[‡]University of the Chinese Academy of Sciences, Beijing 100049, P. R. China

ABSTRACT: Eu^{2+}-doped $SrSi_2O_2N_2$ has recently been identified as a viable green phosphor that in conjunction with a blue-emitting diode can be used in solid-state white-lighting sources. In this study, we attempt to improve the photoluminescence and thermal quenching behavior by codoping Re^{3+} (Re = La, Gd, Y, Dy, Lu, Sc) and Li^+ instead of Sr^{2+}. Trivalent cation substitution at the Sr^{2+} site enhances the photoluminescence intensities and also achieves better thermal stability at high temperature. The lifetime decay properties in the related substituted phosphors are investigated. Furthermore, under the 460 nm blue light irradiation, this green phosphor exhibits excellent luminescence properties with absorption and internal/external efficiencies. High-color-rendition warm-white LEDs using the phosphor have the color temperature and color rendition of 4732 K and 91.2, respectively, validating its suitability for use in solid-state white lighting.

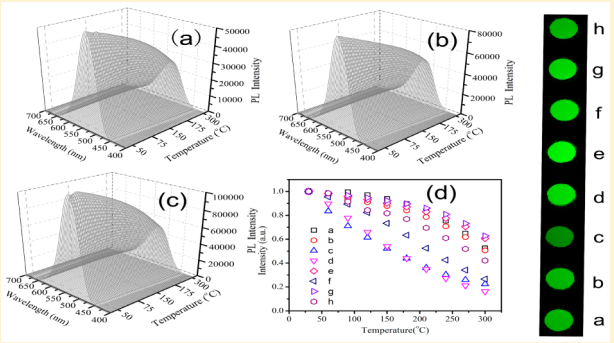

INTRODUCTION

Recently, white-light-emitting diodes (LEDs) are proposed to take the place of conventional light sources to be a new generation light source bulbs because of their many advantages in energy efficiency, long lifetime, environmental friendliness.[1−4] In order to improve the performance and energy-saving potential of pc-LEDs, it is important to develop new high-efficiency phosphors as well as to improve the properties of existing materials.[5−8] Various luminescent solid-state materials with emission from the blue to the red spectral region have been described.[9−15] Among the developed phosphors, the compounds containing N element such as nitrides and oxynitrides have attracted much more attention due to their outstanding chemical stability and high luminescence efficiency.[16−28]

Promising green phosphors $SrSi_2O_2N_2:Eu^{2+}$ need to efficiently absorb in the near UV to blue spectral range, allowing them to be used as down-conversion luminescent materials for white-light LEDs. Extensive research has been attempted to enhance the luminescence intensity of $SrSi_2O_2N_2:Eu^{2+}$ by controlling synthesis parameters or codoping with Dy^{3+}, Mn^{2+}, and/or Ce^{3+}.[29−33] However, Lee et al. reported that Mg^{2+}-substituted $SrSi_2O_2N_2:Eu^{2+}$ phosphors had more efficient luminescence and better thermal quenching behavior.[34] More recently, Li et al. reported the continuous luminescence adjustments from green to yellow are observed with gradual replacement of Sr^{2+} with Ba^{2+}.[35]

In the work reported here, various rare earth ions Re^{3+} (Re = La, Gd, Y, Dy, Lu, Sc) and Li^+ were individually substituted into the Sr^{2+} sites. The effect of substitution of Sr^{2+} by Re^{3+} and Li^+ on the luminescence properties of $SrSi_2O_2N_2:Eu^{2+}$ were investigated. Accordingly, we propose the underlying mechanisms of the changes in the photoluminescence properties by the substitution. The influence of the substitution on the thermal quenching is investigated. The suitability of the phosphor in solid-state lighting is also testified by combining it to a blue LED chip, and the optical properties of the device are presented.

EXPERIMENTAL SECTION

Synthesis. The powder phosphor samples ($SrSi_2O_2N_2:Eu^{2+},Re^{3+},Li^+$ (Re = La, Gd, Y, Dy, Lu, Sc)) were synthesized by the conventional solid-state reaction in one step. $SrCO_3$ (A.R. (Analytical Reagent)), a-Si_3N_4 (Alfa Aesar), and Eu_2O_3(99.99%) were used as starting materials. Appropriate amounts of starting powders with the Sr to Si ratio of 1:2.1 were weighed out and mixed in an alumina mortar. The powder mixture was mixed homogeneously by an agate mortar for 30 min, placed in a crucible with a lid, and then sintered in a tubular furnace at 1400 °C for 4 h in reductive atmosphere (10% H_2 + 90% N_2 mixed flowing gas).

Received: June 22, 2015
Published: September 2, 2015

DOI: 10.1021/acs.inorgchem.5b01402
Inorg. Chem. 2015, 54, 9060−9065

Characterization. The phase purity of all samples were identified by powder X-ray diffraction (XRD) analysis (Bruker AXS D8), with graphite monochromatized Cu Kα radiation (λ = 0.15405 nm) operating at 40 kV and 40 mA. The measurements of the photoluminescence (PL), photoluminescence excitation (PLE), and diffuse reflectance (DR) spectra were performed with a Hitachi F-7000 spectrometer equipped with a 150 W xenon lamp as the excitation source. White $BaSO_4$ (reflection 100%) was used as the standard reference for reflection measurement. Absolute photoluminescence quantum yields (QYs) were measured by the absolute PL quantum yield measurement system (Quantaurus-QY, Hamamatsu Photonics K. K., Japan). The luminescence decay curves were obtained from a Lecroy Wave Runner 6100 digital oscilloscope (1 GHz) using a tunable laser (pulse width = 4 ns, gate = 50 ns) as the excitation source (Continuum Sunlite OPO). The Commission Internationale de l'Eclairage (CIE) chromaticity color coordinates, color rendering index (Ra), and color temperature (CCT) were measured by Starspec SSP6612.

RESULTS AND DISCUSSION

When doped with rare earth ions, an equal amount of Li^+ had to be added for the charge compensation. The doping mechanism should be $Re^{3+} + Li^+ = 2Sr^{2+}$. The prepared $Sr_{0.95}Si_2O_2N_2$:0.05Eu^{2+}; $Sr_{0.95}Si_2O_2N_2$:0.05Eu^{2+},0.2Li^+; and $Sr_{0.55}Si_2O_2N_2$:0.05Eu^{2+},0.2Re^{3+},0.2Li^+ (Re = La, Gd, Y, Dy, Lu, Sc) were labeled as a, b, c, d, e, f, g, and h, respectively. All the prepared samples were characterized by the powder X-ray diffraction to verify their phase purity. Figure 1 shows the typical powder XRD patterns of $Sr_{0.95}Si_2O_2N_2$:0.05Eu^{2+}; $Sr_{0.95}Si_2O_2N_2$:0.05Eu^{2+},0.2Li^+; and $Sr_{0.55}Si_2O_2N_2$:0.05Eu^{2+},0.2Re^{3+},0.2Li^+ samples. It can be seen that all the XRD patterns are well-matched with the $SrSi_2O_2N_2$ phase. The doping of Li^+ and lanthanide ions does not induce any other distinct impurity phases, indicating the successful incorporation of these rare earth ions into the $SrSi_2O_2N_2$ host. In addition, the diffraction peaks of $Sr_{0.55}Si_2O_2N_2$:0.05Eu^{2+},0.2Re^{3+},0.2Li^+ (Re = Y, Lu, Dy and Sc) are shifted obviously to higher angles with respect to those of standard $Sr_{0.95}Si_2O_2N_2$:0.05Eu^{2+}. Previous study revealed that the real structure of $SrSi_2O_2N_2$ is triclinic structure (space group P1, a = 7.0802(2) nm, b = 7.2306(2) nm, c = 7.2554(2) nm, α = 88.767(3), β = 84.733(2), γ = 75.905(2), and V = 358.73(2) nm^3, Z = 4). There are four different Sr^{2+} crystallographic sites in the triclinic $SrSi_2O_2N_2$ unit cell, and each Sr^{2+} ion is coordinated with six O and two N atoms to form a trigonal prism.[36] As we know, the ionic radius of rare earth ions is almost in the order of $La^{3+} > Gd^{3+} > Y^{3+} > Dy^{3+} > Lu^{3+} > Sc^{3+}$, which is 1.16, 1.05, 1.04, 1.03, 0.98, and 0.86 Å. respectively, with CN = 8. This is because the radius of Sr^{2+} (1.26 Å for CN = 8) is much bigger than that of Re^{3+} (Re = Y, Lu, Dy, and Sc), showing that Re^{3+} has been effectively incorporated into the $Sr_{0.95}Si_2O_2N_2$:0.05Eu^{2+} host lattice. Figure 2 presents the typical SEM images of samples. It is clearly seen that nearly all of the Li^+ doped powders showed crystallites of up to ~5 μm, compared to <3 μm for the undoped phosphor. These results indicated that doping Li^+ can enhance the crystallinity and particle sizes of the resultant powder. Notably, the sample with adding Li^+ and La^{3+} has small particle size, and the particle is not crystallized very well compared with the other samples. The corresponding EDX spectrum analysis (Figure 2I) indicates that the product has a chemical composition of Sr, Si, O, and N and that no impurity elements are present.

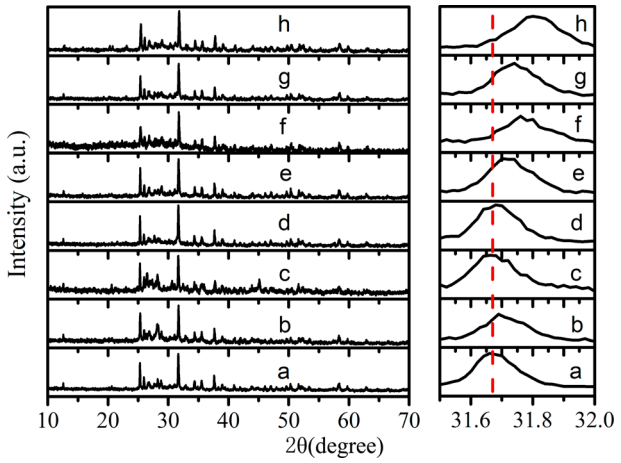

Figure 1. XRD patterns of the as-prepared $Sr_{0.95}Si_2O_2N_2$:0.05Eu^{2+}; $Sr_{0.95}Si_2O_2N_2$:0.05Eu^{2+},0.2Li^+; and $Sr_{0.55}Si_2O_2N_2$:0.05Eu^{2+},0.2Re^{3+},0.2Li^+ samples.

The PLE and PL spectra of $Sr_{0.95}Si_2O_2N_2$:0.05Eu^{2+}; $Sr_{0.95}Si_2O_2N_2$:0.05Eu^{2+},0.2Li^+; and $Sr_{0.55}Si_2O_2N_2$:0.05Eu^{2+},0.2Re^{3+},0.2Li^+ (Re = La, Gd, Y, Dy, Lu, Sc) phosphors are presented in Figure 3a, where each spectrum is normalized at the maximum of the spectral intensity. The PL spectra present a green emission band peaking at 535 nm due to Eu^{2+} $4f^65d - 4f^7$ transition, of which the position and the shape keep unchanged for various rare earth ions doped. Contrast to the PL, the excitation bands of all the phosphors with rare earth ions doping have a red-shift tendency. Such a slight red-shift behavior should be attributed to the variation of the crystal environment energy of f−d transition of Eu^{2+} modified by Re/Sr replacement in the crystal lattice. Figure 3b exhibits the values of the relative intensity of different samples. Codoping with Li^+ has become a common method for improving optical efficiency in luminescent materials.[37−40] For this reason, the product $Sr_{0.95}Si_2O_2N_2$:0.05Eu^{2+}, 0.2Li^+ has been synthesized and compared by PL intensity. In this system, Li^+ can improve luminescence via a flux effect leading to larger crystallites. However, we have observed that the enhancement effect of Re^{3+},Li^+ codoping is far superior to that of Li^+ single doped, and introduction of Y, Dy, and Lu ions into the $SrSi_2O_2N_2$:0.05Eu^{2+}, Li^+ structure increased the most effective intensity from all used Re^{3+} dopants. Upon the addition of Lu^{3+} to $SrSi_2O_2N_2$:0.05Eu^{2+}, Li^+, the PL intensity can be intensified by up to 80% as Figure 3b shows. Only the addition of La decreases the emission intensity. This phenomenon can be ascribed to the two reasons. First, Li^+ ions can act as the flux for preparing the $SrSi_2O_2N_2$:Eu^{2+} phosphor, which enhances the crystallinity and particle morphology of the resultant powder. Larger crystallites with higher phase purity are produced, as evidenced by SEM images from Figure 2. Second, Li^+ codoping helps to incorporate the Re^{3+} into Sr^{2+} sites by compensating for the different charges between Re^{3+} and Sr^{2+}. In the view of effective ionic radii, [Sr^{2+} (1.26 Å), La^{3+} (1.16 Å), Gd^{3+} (1.05 Å), Y^{3+} (1.04 Å), Dy^{3+}(1.03 Å), Lu^{3+} (0.98 Å), and Sc^{3+} (0.86 Å)], it is believed that the smaller ions make the Re substitution more easier with Li^+ help.

DOI: 10.1021/acs.inorgchem.5b01402
Inorg. Chem. 2015, 54, 9060−9065

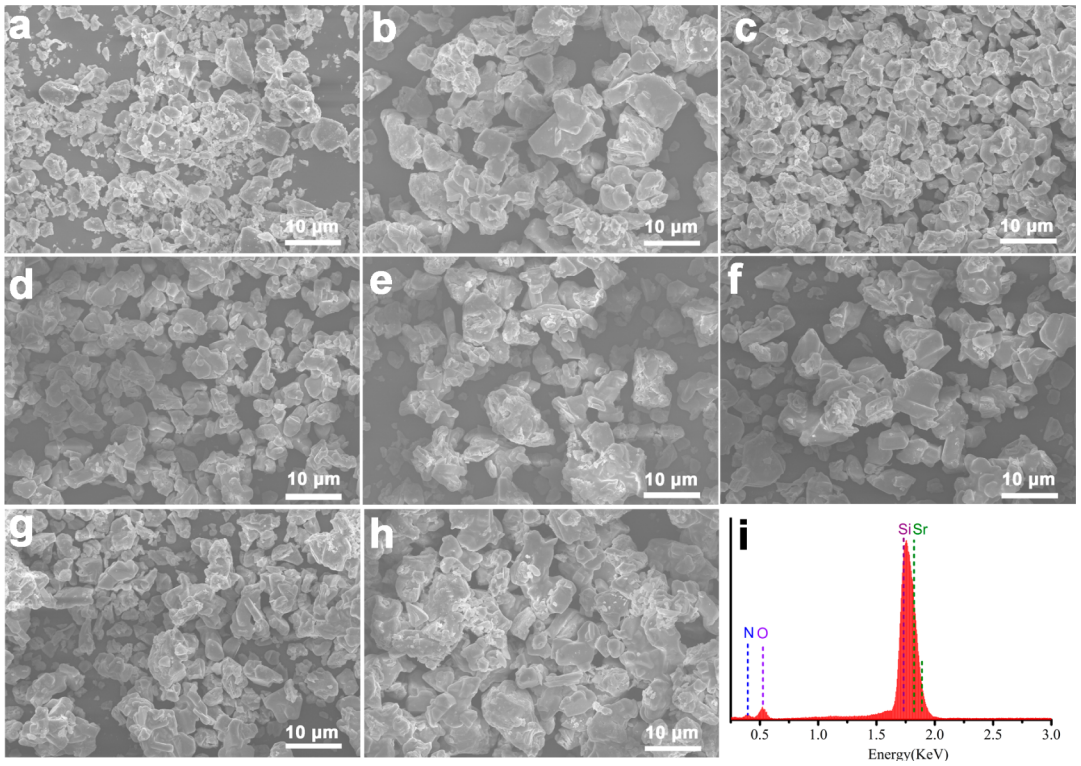

Figure 2. Typical SEM images of different samples (a–h) and the EDX spectrum of $Sr_{0.95}Si_2O_2N_2$:0.05Eu^{2+} phosphor (I).

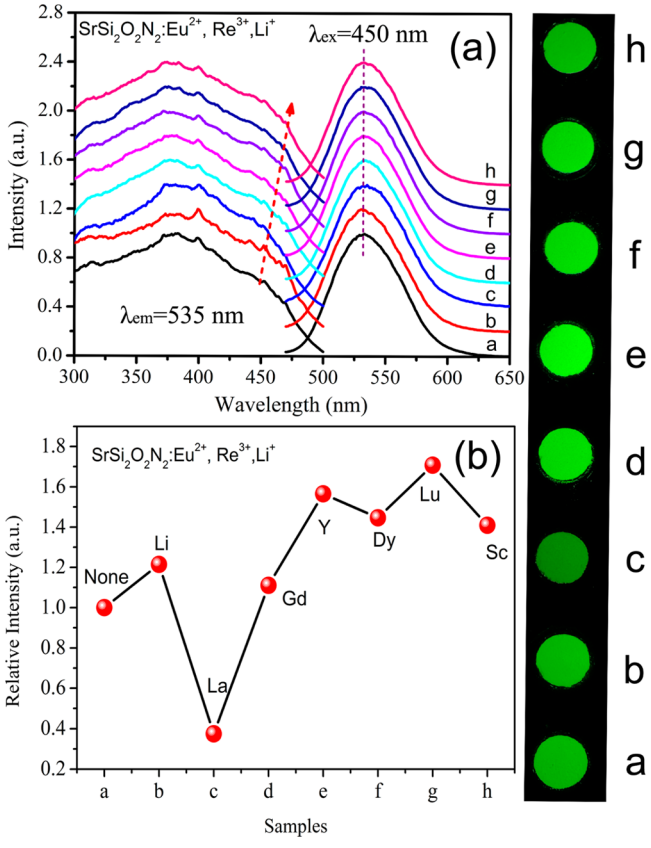

Figure 3. Normalized PLE and PL spectra (a) and the values of the relative intensity (b) of $Sr_{0.95}Si_2O_2N_2$:0.05Eu^{2+}; $Sr_{0.95}Si_2O_2N_2$:0.05Eu^{2+},0.2Li^+; and $Sr_{0.55}Si_2O_2N_2$:0.05Eu^{2+},0.2Re^{3+},0.2Li^+ (Re = La, Gd, Y, Dy, Lu, and Sc) phosphor.

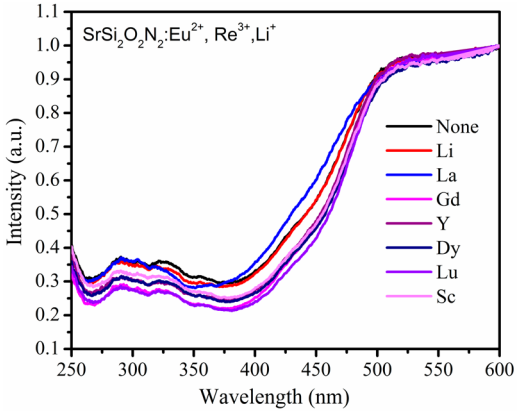

Figure 4. Diffuse reflectance spectra of our prepared samples.

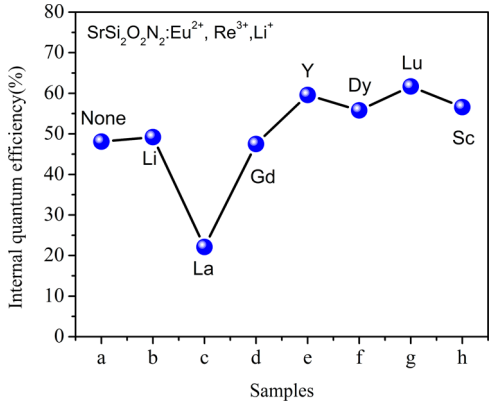

Figure 5. Internal quantum efficiency of $Sr_{0.95}Si_2O_2N_2$:0.05Eu^{2+},0.2Li^+ with doping different Re^{3+} ions.

DOI: 10.1021/acs.inorgchem.5b01402
Inorg. Chem. 2015, 54, 9060−9065

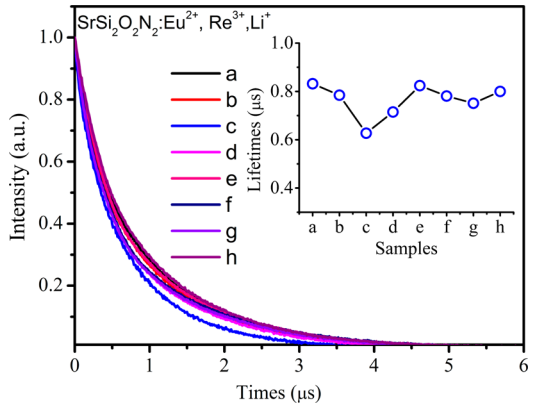

Figure 6. Typical luminescence decay curves of our samples under the excitation of 330 nm. The inset is the fluorescence lifetimes of samples.

As we know, the PL intensity is determined by two factors, the absorption efficiency for excitation light and internal quantum efficiency including transferring excitation energy to activator and subsequent emitting.[41] To understand which of the two factors results in luminescent properties, the diffuse reflection spectra are measured for various samples first. Figure 4 depicts typical diffuse reflection spectra of the $Sr_{0.95}Si_2O_2N_2$:0.05Eu^{2+}; $Sr_{0.95}Si_2O_2N_2$:0.05Eu^{2+},0.2Li^+; and $Sr_{0.55}Si_2O_2N_2$:0.05Eu^{2+},0.2Re^{3+},0.2Li^+ (Re = La, Gd, Y, Dy, Lu, Sc) phosphors. With the exception of doping La^{3+} ions, all doping ions enhanced the absorption of $SrSi_2O_2N_2$:Eu^{2+}. Notably, doping La^{3+} ions completely reduced the absorption. Although the origin of this phenomenon remains unclarified at present, in this case, it is speculated that some defects are formed due to the addition of La^{3+}. These defects may act as absorbers to compete with Eu^{2+} so as to reduce the absorbance of Eu^{2+} and then PL intensity. The effect of the doping ions on the internal quantum efficiency of the green phosphors is shown in Figure 5. Upon the blue light irradiation, the change of internal quantum efficiency with the different ions is consistent with that of the relative intensity from Figure 3b. However, the internal quantum efficiency increases by 28% from 48.4% to 61.7% after codoping Lu^{3+} ions, this value is not consistent with that of 80% determined from PL measurements. The reason for this difference can be explained by the different variations of absorption efficiency. Figure 6 shows the typical luminescence decay curves of our samples under the excitation of 330 nm. It is found that the lifetimes of the samples do not change obviously with Re substitution except for the La and Gd ions doping. The lifetime τ is dominated by the radiative transition rate W_R, and the nonradiative decay rate W_{NR}, which can be written as $\tau = 1/(W_R + W_{NR})$, and internal quantum efficiency(η) is based on the relationship $\eta = W_R/(W_R + W_{NR})$. When La^{3+} and Gd^{3+} is built into $Sr_{0.55}Si_2O_2N_2$:0.05Eu^{2+},0.2Li^+, both the lifetimes and internal quantum efficiency reduce. Although the ionic radius of La and Gd is closer to that of Sr, substitution of Sr by Li, La/Gd may increase any defects in the host lattice or make the crystallinity of the phosphor worse. Therefore, we demonstrated that the nonradiative rate increases greatly with La^{3+} and Gd^{3+} substitution at the Sr^{2+} site, leading to the luminescence efficiency reduction.

The thermal quenching property is one of the important technological parameters for phosphors used in solid-state

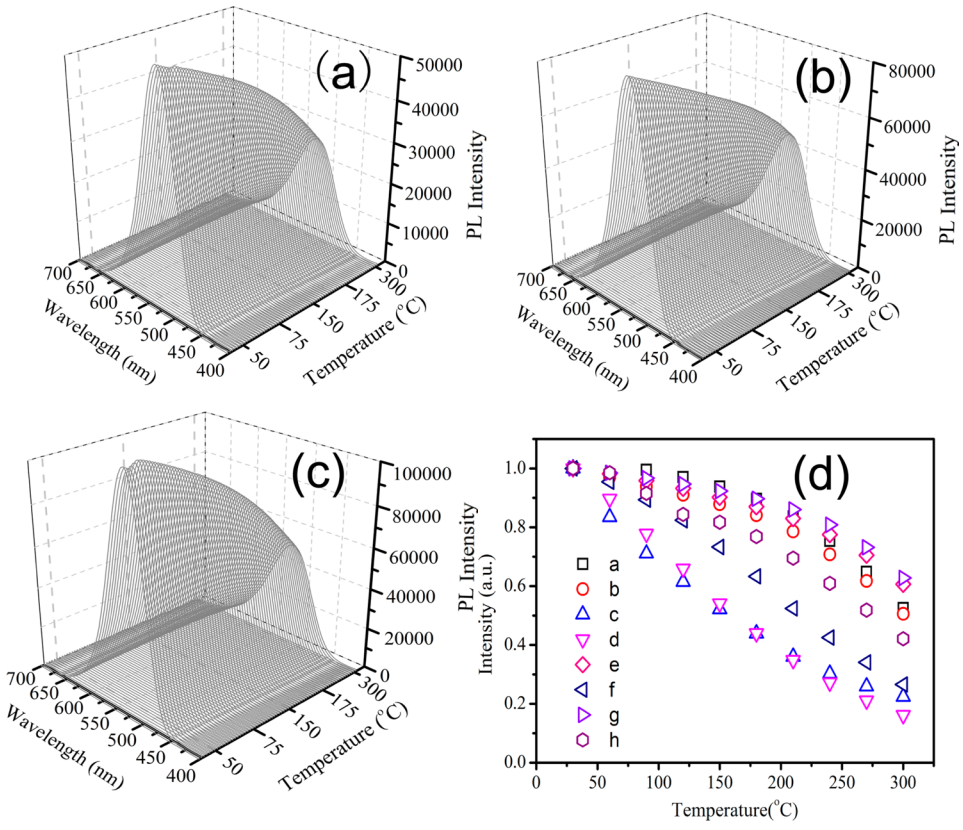

Figure 7. Three-dimensional temperature-dependence PL emission spectra of a (a), e (b) g (c) and thermal quenching behavior of samples (d) excited by 365 nm UV light.

DOI: 10.1021/acs.inorgchem.5b01402
Inorg. Chem. 2015, 54, 9060−9065

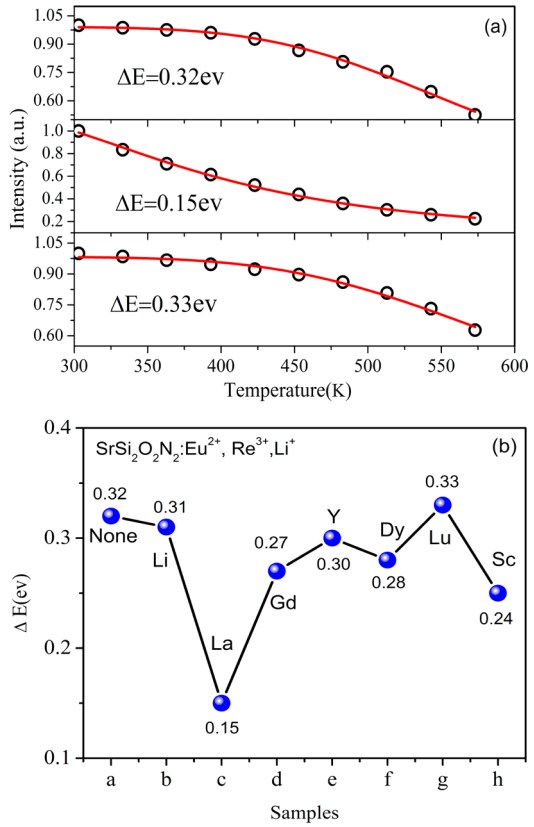

Figure 8. (a) Temperature dependence of PL intensity of Eu^{2+} in $Sr_{0.95}Si_2O_2N_2$:0.05Eu^{2+}; $Sr_{0.55}Si_2O_2N_2$:0.05Eu^{2+},0.2La^{3+},0.2Li^{+}; and $Sr_{0.55}Si_2O_2N_2$:0.05Eu^{2+},0.2Lu^{3+},0.2Li^{+} under excitation at 365 nm. The black dots are experimental data, and the red lines are fitting functions. (b) Activation energy values of different samples.

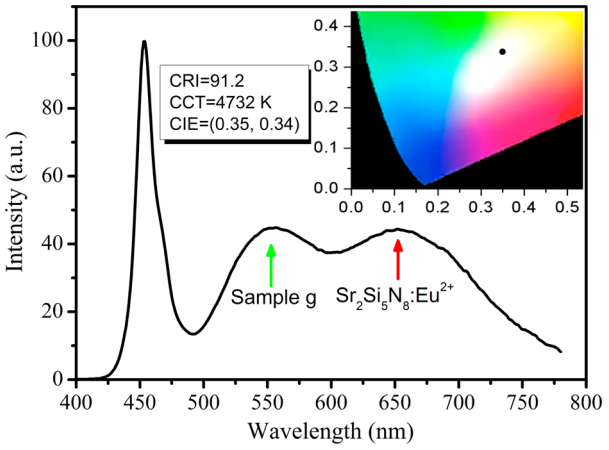

Figure 9. EL spectrum of white emitting LEDs composed of a 460 nm blue chip and a phosphor blend of $Sr_2Si_5N_8$:Eu^{2+} and $Sr_{0.55}Si_2O_2N_2$:0.05Eu^{2+},0.2Lu^{3+},0.2Li^{+}. Insets show the CIE chromaticity diagram of white LEDs.

lighting because it has considerable influence on the light output and color rendering index. The 3D temperature-dependence PL emission spectra of a, e, g and thermal quenching behavior of papered phosphors excited by 365 nm UV light are illustrated in Figure 7. The emission intensities of all samples gradually decline. The decrease in emission intensity with increasing temperature originates from a temperature-dependent phonon-coupling factor, which can be explained by thermal quenching at configurational coordinate diagram.[42] The excited luminescent center is thermally activated through phonon interaction and then thermally released through the crossing point between the excited state and the ground state. It is noted that the emission intensity of $Sr_{0.95}Si_2O_2N_2$:0.05Eu^{2+} decreases slower with increasing temperature than that of $Sr_{0.55}Si_2O_2N_2$:0.05Eu^{2+},0.2Re^{3+},0.2Li^{+} (Re = La, Gd, and Dy) but faster than that of $Sr_{0.55}Si_2O_2N_2$:0.05Eu^{2+},0.2Re^{3+},0.2Li^{+} (Re = Y and Lu) phosphor. This indicates that the doping of Y^{3+} and Lu^{3+} is an advantage to the thermal stability. Especially, upon heating the phosphor samples in a temperature range from 150 to 300 °C, the $Sr_{0.55}Si_2O_2N_2$:0.05Eu^{2+},0.2Re^{3+},0.2Li^{+} (Re = Y and Lu) has a comparatively good temperature quenching effect. This behavior is understood in terms of two reasons: on the one hand, in the configurational coordinate diagram, in the case of $Sr_{0.95}Si_2O_2N_2$:0.05Eu^{2+} to $Sr_{0.55}Si_2O_2N_2$:0.05Eu^{2+},0.2Re^{3+},0.2Li^{+} (Re = Y and Lu), an activation energy increases, leading to increasing the non-radiative barrier from the excited state to the ground state; consequently, the samples are quenched at higher temperature. On the other hand, the vibrational frequency will decrease as Sr^{2+} ions are substituted by Re^{3+}, Li^{+} (Re = Y and Lu) ions. The lower vibrational frequency prevents the crossover relaxation from the excited state to the ground state. According to the classical theory of thermal quenching, the temperature-dependent PL intensity can be described by the equation[43]

$$I(T) = \frac{I(0)}{1 + A\exp(-\Delta E/k_B T)} \quad (1)$$

Here $I(0)$is the initial emission intensity of the phosphor at room temperature, $I(T)$ is the emission intensity at different temperatures. A is a constant, ΔE is the activation energy for thermal quenching, and k is the Boltzmann constant. The experimental data are well fitted by eq 1, as shown in Figure 8a. Activation energy values of different samples are shown in Figure 8b. Here, activation energy of Eu^{2+} in $Sr_{0.95}Si_2O_2N_2$ is 0.32 eV. This value is slightly lower than that of Eu^{2+} in $Sr_{0.55}Si_2O_2N_2$:0.05Eu^{2+},0.2Lu^{3+},0.2Li^{+}.

The suitability of the $Sr_{0.55}Si_2O_2N_2$:0.05Eu^{2+},0.2Lu^{3+},0.2Li^{+} green phosphor in white LEDs was also testified in this work. White LED lamps were fabricated using a 460 nm blue chip combined with a blend of red-emitting $Sr_2Si_5N_8$:Eu^{2+} and our prepared phosphors. Figure 9 shows the electroluminescence spectrum of a white LED driven at a 20 mA current. The lamp has a correlated color temperature (CCT) of 4732 K, color rendering index (Ra) of 91.2, and CIE chromatic coordinates (x, y) of (0.35, 0.34). These results demonstrate that $Sr_{0.55}Si_2O_2N_2$:0.05Eu^{2+},0.2Re^{3+},0.2Li^{+} has strong potential applications in developing highly efficient, thermally stable warm white LEDs.

CONCLUSIONS

In summary, the present work demonstrates the effect of codoping Re^{3+} (Re = La, Gd, Y, Dy, Lu, Sc) and Li^{+} instead of Sr^{2+} on the luminescence properties of $SrSi_2O_2N_2$:Eu^{2+} phosphors. The photoluminescence intensity of the $SrSi_2O_2N_2$:Eu^{2+} phosphor is significantly increased as introduction of Y, Dy and Lu ions into the $SrSi_2O_2N_2$:0.05Eu^{2+}, Li^{+} structure. The enhanced PL intensity should have been influenced by the absorption and internal quantum efficiency. Also, thermal stability study of the $SrSi_2O_2N_2$:Eu^{2+},Re^{3+},Li^{+} (Re = La, Gd, Y, Dy, Lu, Sc) phosphors are investigated. Studies

DOI: 10.1021/acs.inorgchem.5b01402
Inorg. Chem. 2015, 54, 9060−9065

have shown that the introduction of a certain amount of Lu could improve thermal stability. Warm white light with high color rendering index has been created by combining the synthesized $SrSi_2O_2N_2$: Eu^{2+},Lu^{3+},Li^+ phosphor with $Sr_2Si_2N_8$:Eu^{2+} and the blue InGaN LED chip, indicative of a promising green phosphor for high efficiency and high reliability solid state lighting.

AUTHOR INFORMATION

Corresponding Authors

*E-mail: hpyou@ciac.ac.cn. Fax: +86-431-85698041. Tel: +86-431-85262798.

*E-mail: wlv@ciac.ac.cn.

Notes

The authors declare no competing financial interest.

ACKNOWLEDGMENTS

This work is financially supported by the National Natural Science Foundation of China (Grant Nos. 11304309 and 51472236), the National Basic Research Program of China (973 Program, Grant No. 2014CB643803), and the Fund for Creative Research Groups (Grant No. 21221061).

REFERENCES

(1) Nakamura, S.; Mukai, T.; Senoh, M. *Appl. Phys. Lett.* **1994**, *64*, 1687−1689.

(2) Feldmann, C.; Jüstel, T.; Ronda, C. R.; Schmidt, P. J. *Adv. Funct. Mater.* **2003**, *13*, 511−516.

(3) Oh, J. H.; Yang, S. J.; Do, Y. R. *Light: Sci. Appl.* **2014**, *3*, e141.

(4) Shang, M. M.; Li, C. X.; Lin, J. *Chem. Soc. Rev.* **2014**, *43*, 1372−1386.

(5) Denault, K. A.; Brgoch, J.; Gaultois, M. W.; Mikhailovsky, A.; Petry, R.; Winkler, H.; DenBaars, S. P.; Seshadri, R. *Chem. Mater.* **2014**, *26*, 2275−2282.

(6) Liu, Y. F.; Zhang, X.; Hao, Z. D.; Liu, X. Y.; Wang, X. J.; Zhang, J. H. *J. Mater. Chem.* **2011**, *21*, 6354−6358.

(7) Shang, M. M.; Fan, J.; Lian, H. Z.; Zhang, Y.; Geng, D. L.; Lin, J. *Inorg. Chem.* **2014**, *53*, 7748−7755.

(8) Luo, Y.; Xia, Z. G. *J. Phys. Chem. C* **2014**, *118*, 23297−23305.

(9) Liu, C.; Qi, Z.; Ma, C. G.; Dorenbos, P. R.; Hou, D.; Zhang, S.; Kuang, X.; Zhang, J.; Liang, H. *Chem. Mater.* **2014**, *26*, 3709−3715.

(10) Li, W. Y.; Xie, R. J.; Zhou, T. L.; Liu, L. H.; Zhu, Y. J. *Dalton Trans.* **2014**, *43*, 6132−6138.

(11) Li, X. F.; Budai, J. D.; Liu, F.; Howe, J. Y.; Zhang, J. H.; Wang, X. J.; Gu, Z. J.; Sun, C. J.; Meltzer, R. S.; Pan, Z. W. *Light: Sci. Appl.* **2013**, *2*, e50−e58.

(12) Zhu, H. M.; Lin, C. C.; Luo, W.; Shu, S.; Liu, Z.; Liu, Y.; Kong, J.; Ma, E.; Cao, Y.; Liu, R. S.; Chen, X. *Nat. Commun.* **2014**, *5*, 4312.

(13) Pust, P.; Wochnik, A.; Baumann, S. E.; Schmidt, P. J.; Wiechert, D.; Scheu, C.; Schnick, W. *Chem. Mater.* **2014**, *26*, 3544−3549.

(14) Wang, C. Y.; Xie, R. J.; Li, F. Z.; Xu, X. *J. Mater. Chem. C* **2014**, *2*, 2735−2742.

(15) Gwak, S. J.; Arunkumar, P.; Im, W. B. *J. Phys. Chem. C* **2014**, *118*, 2686−2692.

(16) Hirosaki, N.; Xie, R. J.; Kimoto, K.; Sekiguchi, T.; Yamamoto, Y.; Suehiro, T.; Mitomo, M. *Appl. Phys. Lett.* **2005**, *86*, 211905−1−3.

(17) Xie, R. J.; Hirosaki, N.; Suehiro, T.; Xu, F. F.; Mitomo, M. *Chem. Mater.* **2006**, *18*, 5578−5583.

(18) Uheda, K.; Hirosaki, N.; Yamamoto, Y.; Naito, A.; Nakajima, T.; Yamamoto, H. *Electrochem. Solid-State Lett.* **2006**, *9*, H22−H25.

(19) Bachmann, V.; Jüstel, T.; Meijerink, A.; Ronda, C.; Schmidt, P. J. *J. Lumin.* **2006**, *121*, 441−449.

(20) Xie, R. J.; Hirosaki, N.; Li, H. L.; Li, Y. Q.; Mitomo, M. *J. Electrochem. Soc.* **2007**, *154*, J314.

(21) Li, Y. Q.; Hirosaki, N.; Xie, R. J.; Takeda, T.; Mitomo, M. *Chem. Mater.* **2008**, *20*, 6704−6714.

(22) Kimoto, K.; Xie, R. J.; Matsui, Y.; Ishizuka, K.; Hirosaki, N. *Appl. Phys. Lett.* **2009**, *94*, 041908−1−3.

(23) Bachmann, V.; Ronda, C.; Oeckler, O.; Schnick, W.; Meijerink, A. *Chem. Mater.* **2009**, *21*, 316−325.

(24) Oeckler, O.; Kechele, J. A.; Koss, H.; Schmidt, P. J.; Schnick, W. *Chem. - Eur. J.* **2009**, *15*, 5311−5319.

(25) Liu, L.; Xie, R. J.; Li, W.; Hirosaki, N.; Yamamoto, Y.; Sun, X.; Johnson, D. *J. Am. Ceram. Soc.* **2013**, *96*, 1688−1690.

(26) Suehiro, T.; Hirosaki, N.; Xie, R. J. *ACS Appl. Mater. Interfaces* **2011**, *3*, 811−816.

(27) Zhang, L.; Zhang, J.; Zhang, X.; Hao, Z.; Zhao, H.; Luo, Y. *ACS Appl. Mater. Interfaces* **2013**, *5*, 12839−12846.

(28) Wang, X.; Seto, T.; Zhao, Z.; Li, Y.; Wu, Q.; Li, H.; Wang, Y. *J. Mater. Chem. C* **2014**, *2*, 4476−4481.

(29) Yang, X.; Song, H.; Yang, L.; Xu, X. *J. Am. Ceram. Soc.* **2011**, *94*, 164−171.

(30) Liu, R. S.; Liu, Y. H.; Bagkar, N. C.; Hu, S. F. *Appl. Phys. Lett.* **2007**, *91*, 061119−1−3.

(31) Song, X.; Fu, R.; Agathopoulos, S.; He, H.; Zhao, X.; Li, R. *J. Electrochem. Soc.* **2010**, *157*, J34−J38.

(32) Fei, Q. N.; Liu, Y. H.; Gu, T. C.; Wang, D. J. *J. Lumin.* **2011**, *131*, 960−964.

(33) Song, X.; Fu, R.; Agathopoulos, S.; He, H.; Zhao, X.; Zeng, J. *Mater. Sci. Eng., B* **2009**, *164*, 12−15.

(34) Lee, S. H.; Kim, K. B.; Kim, J. M.; Jeong, Y. K.; Kang, J. G. *Phys. Status Solidi A* **2013**, *210*, 1093−1097.

(35) Li, G.; Lin, C. C.; Chen, W. T.; Molokeev, M. S.; Atuchin, V. V.; Chiang, C. Y.; Zhou, W.; Wang, C. W.; Li, W. H.; Sheu, H. S.; Chan, T. S.; Ma, C.; Liu, R. S. *Chem. Mater.* **2014**, *26*, 2991−3001.

(36) Oeckler, O.; Stadler, F.; Rosenthal, T.; Schnick, W. *Solid State Sci.* **2007**, *9*, 205−212.

(37) Byeon, S. H.; Ko, M. G.; Park, J. C.; Kim, D. K. *Chem. Mater.* **2002**, *14*, 603−608.

(38) Liu, H.; Hao, Y.; Wang, H.; Zhao, J.; Huang, P.; Xu, B. *J. Lumin.* **2011**, *131*, 2422−2426.

(39) Hao, Z. D.; Zhang, X.; Luo, Y. S.; Zhang, L. G.; Zhao, H. f.; Zhang, J. H. *J. Lumin.* **2013**, *140*, 78−81.

(40) Yadav, R. V.; Singh, S. K.; Rai, S. B. *RSC Adv.* **2015**, *5*, 26321−26327.

(41) Lü, W.; Hao, Z. D.; Zhang, X.; Liu, Y. F.; Luo, Y. S.; Liu, X. Y.; Wang, X. J.; Zhang, J. H. *J. Electrochem. Soc.* **2011**, *158*, H124−H127.

(42) Ropp, R. C. *Luminescence and the Solid State*; Elsevier: New York, 1991.

(43) Dorenbos, P. *J. Phys.: Condens. Matter* **2005**, *17*, 8103−8111.

DOI: 10.1021/acs.inorgchem.5b01402
Inorg. Chem. 2015, 54, 9060−9065